

EXPERIMENTAL STUDY OF THE PLANE TURBULENT
WAKE BEHIND AN AEROFOIL WITH PRESSURE GRADIENT

BY

H. A. Heikal
University of Helwan
Faculty of Engineering and Technology
Mattaria-Cairo, Egypt

S.S. Ayad, H.M. Helmy and A.M. Osman
University of Zagazig
Faculty of Engineering, Shoubra - Cairo, Egypt

ABSTRACT

In search of better estimates of the losses in turbo-machinery; the present work considers the effects of pressure gradient on the wake flow behind an isolated airfoil. Once the wake velocity profile is measured or predicted, drag calculations based on the loss of momentum are carried for different values of pressure gradient.

A wind tunnel was designed and constructed to achieve a two-dimensional flow with zero, positive and negative pressure gradients at different undisturbed velocities.

The resulted velocity distribution shows that at the positive pressure gradients, the distributions are flatter, relative to those with zero pressure gradient, the distributions are steeper. Also as the undisturbed velocity increases, the wake decay increases.

The wake parameters are measured downstream of the trailing edge for positive and negative pressure

This work was carried out at the Turbomachinery Laboratory of the Department of Mechanical Power Engineering, Faculty of Engineering and Technology, University of Helwan, Mattaria-Cairo, Egypt.

IV.3.2

gradients and compared with those at zero pressure gradient.

NOMENCLATURE:

a	constant
b	wake width
c_D	total drag coefficient
C	Chord length of the aerofoil
D	Total drag force
H	Shape factor
L	span length of the aerofoil
P	static pressure
u	velocity at distance y from the x- coordination direction (in the flow direction)
u_1	free stream velocity
u_c	velocity at wake centre line
u_∞	undisturbed velocity upstream of the aerofoil.
x	distance from the trailing edge in streamline direction.
y	distance normal to the aerofoil
α	angle of diffuser (or nozzle) of the test section.
B	wake depth
b	wake width
δ^*	displacement thickness
θ	momentum thickness
ρ	density.

INTRODUCTION

The flow in the plane wake behind an aerofoil continues to be one of the most important problems both from fundamental and practical view point.

For most flow around solid bodies, the boundary layer separates from the body surface towards the rear of the body. Downstream of the separation position, the flow is greatly disturbed by large-scale turbulent eddies, and this region of eddying motion is usually known as the wake. It is characterized by a non-zero vorticity on the downstream side of the body even if the upstream flow is uniform. The flow in the wake is a free turbulent

IV.3.3

shear flow with no solid boundaries to control the mean and fluctuation flow patterns. The flow is bounded on both sides by a non-turbulent irrotational flow.

The organized structure of large eddies within the wake produces large gradients of the longitudinal mean velocity component u (in the direction of flow x) with respect to normal distance y and in consequence the turbulent shear stress component associated with $\partial u / \partial y$ is important, while the other shear stress components can be neglected, see figure (1) for the coordinate system. Wake flows within the passages of turbomachines are likely to be under diffuser effects (for compressors) or nozzle effect (for turbines). The decay or growth of the wake is strongly affected by pressure gradients. In a diffusing or a nozzle passage, the flow is nonuniform owing to the wake induced by an obstruction upstream. The overall performance of the diffuser or the nozzle strongly depends on the manner by which the wake decays as the pressure rises or decreases.

If the positive pressure gradient is large enough, the wake may grow rather than decay, so that a zone of stagnant or reversed flow develops.

In a typical gas turbine engine, air leaving an axial flow compressor take out, passes through a diffuser before entering the combustor. Combustor efficiency is strongly affected by the velocity profile at the diffuser exit. Werle and Verdon [1]* gave detailed numerical calculation on the flow passed symmetric trailing edges.

The decay of turbulent wake in zero-pressure gradient flow have been studied by a number of investigators including Schlichting [2], Townsend[3] and many other authors [4-6]. Measurements for a wake with pressure gradient were made by Kearney[7].

It is important to study wake characteristics in an aerodynamic field, as this study may yield a

* Number in square parenthesis refer to reference listings.

better procedure for calculating drag of a body situated in the free shear flow with positive or negative pressure gradient and thus better estimates of losses in turbomachinery.

EXPERIMENTAL SET UP

An open circuit wind tunnel was constructed to obtain two-dimensional flow with positive, negative, and zero pressure gradients at the test section, as shown in figure (2). The inlet section is designed to obtain minimum disturbance using a bell mouth shape, with a convergent squared cross-section. At a distance of 200 mm downstream from the end of inlet section, a honeycomb of length 150 mm is located. The airfoil is located horizontally at 900 mm downstream of the honeycomb directly before the working section. The working section dimensions are 1230 x 305 x 305 mm at zero pressure gradient. The working section has two movable sides, to produce positive, and negative pressure gradients. A valve is located downstream of the fan, to regulate the discharge. The wake generator, is a straight airfoil, with 22 mm maximum thickness and its chord length is 150 mm. The velocity profiles of the wake is measured at a nondimensional $x/c = 0.067, 0.867, 1.667$ and 2.467 downstream of the airfoil by using a three-hole cylindrical probe.

EXPERIMENTAL RESULTS

Since the problem of wake at zero pressure gradient is well investigated, a special attention will be paid to the effect of pressure gradient on the wake shape. The zero pressure gradient measurements were done to check the characteristics of the test rig and to be used as a reference for comparison with the measurements at both positive and negative pressure gradients.

Throughout the results the wake width is measured experimentally from the velocity distribution. For the accuracy, the half value width (this is the distance from the axis of symmetry, at which the mean velocity difference is half the maximum value) is used. The relative wake depth β is

defined as:

$$\beta = \frac{u_1 - u_c}{u_1}$$

where, u_1 : free stream velocity.
 u_c : velocity at the wake centre line.

The velocity distributions are measured at different distance from the trailing edge and different undisturbed velocities for zero, positive and negative pressure gradients as shown in figures (3), (4) and (5) respectively. The figures show that, the wake depth decreases and the wake width increases as the distance from the trailing edge, increases downstream of the wake generator.

The flow pattern at zero pressure gradient is different from that with pressure gradients, because the free stream lines at zero pressure gradient are parallel, but they diverge for positive pressure gradients or converge for negative pressure gradients.

When the positive pressure gradient increases the wake width increases and becomes flatter at the wake centre. On the other hand, as the negative pressure increases, the wake shape becomes more sharper as compared with the case of zero-pressure gradient.

The wake decay at negative pressure gradient is rapid and thus both the wake depth and wake width are smaller than those with zero and positive pressure gradients. These results can be explained by the reenergizing process. The reenergizing process is very quick and consequently the wake decay is very rapid.

Figure (6) shows the free stream velocity distributions (u/u_{10}) in the direction of flow at zero, positive and negative pressure gradients. The variation of the velocity along the distance from the trailing edge is a linear relation. This relation can be expressed by Hill [8] equation.

$$\frac{u_1}{u_{10}} = 1 + a \frac{\beta_0^2 x}{\theta_0} \quad (1)$$

where β_0 & θ_0 are the wake depth and the momentum thickness at first station.

a is constant depending on the angle of the diffuser or the nozzle.

The effect of pressure gradients on the relative wake depth is shown in figure (7). The positive pressure gradient causes an increase of the dimensionless wake depth β till $\alpha = 12^\circ$ to 14° and then it slightly decreases with further increasing of the positive pressure gradient. This behaviour is due to the separation which occurs at $\alpha = 14^\circ$.

In order to compare the measured values of relative wake depth B with those calculated by Hill [8], the Von Karman momentum integral equation is used together with the transverse velocity distribution at the same conditions.

$$\frac{u_1 - u}{u_1} = \frac{B}{2} \left(1 + \cos \frac{\pi y}{\delta} \right) \quad (2)$$

where δ is half of the wake width at free stream.

The Von Karman momentum equation is:

$$\frac{d\theta}{dx} + (2 + H) \frac{\theta}{u_1} \frac{du_1}{dx} = 0 \quad (3)$$

Substituting from free stream longitudinal velocity equation (1) into the wake depth equation by Hill

IV.3.7

$$\frac{P}{P_0} = \left(\frac{u_{10}}{u_1}\right)^2 \left[1 + \frac{8\pi^2}{\pi^2-4} \left(\frac{\epsilon}{u_1\theta}\right) \int_{x_0}^x \frac{u_{10}}{u_1} d\left(\frac{P_0^2 x}{\theta}\right)^{-\frac{1}{2}} \right] \dots\dots\dots (4)$$

and integrating from $x_0 = 10$ mm to x , where x_0 is the distance between the first station and the trailing edge of the airfoil in mm, we get.

$$\frac{P}{P_0} = \left[1 - a \left(\frac{P_0^2 x}{\theta}\right)^{-\frac{1}{2}} \right]^{-2} \left[1 + \frac{8\pi^2}{a(\pi^2-4)} \frac{\epsilon}{u_1\theta} \ln\left(\frac{1+a\frac{P_0^2 x}{\theta}}{1+10\frac{P_0^2 a}{\theta}}\right) \right]^{-\frac{1}{2}} \dots\dots\dots (5)$$

where ϵ is the eddy viscosity.

This equation is suitable for positive and negative pressure gradients, but for zero pressure gradient, we substitute u_{10}/u_1 equal to unity in equation (4) and integrating from $x_0 = 10$ mm to x we get.

$$\frac{P}{P_0} = \left[1 + \frac{8\pi^2}{\pi^2-4} \left(\frac{\epsilon}{u_1\theta}\right) \left(\frac{P_0^2 x}{\theta} - \frac{10 P_0^2}{\theta}\right)^{-\frac{1}{2}} \right]^{-2} \dots\dots\dots (6)$$

Schlichting [2] showed experimentally that in the constant pressure wake behind a cylinder, the eddy viscosity could be considered constant along the axis of flow.

IV.3.8

Schlichting result can be expressed in the form

$$\frac{\epsilon}{u_1 \theta} = 0.044$$

Hill [8] showed that the value ($\epsilon/u_1 \theta$) may be assumed constant for all pressure gradients. This assumption is quite compatible with the present experimental data as shown in figure (8) to (10). These figures show comparisons between the calculated wake depth from equation (5) or (6) and the present wake depth for the same conditions.

Figure (11) shows the effect of pressure gradient on the relative wake width (b/b_0). The figure shows that the wake width increase with the increase of the pressure gradient and decreases with the negative pressure gradient. Figure (12) and (13) show the variations of momentum thickness θ and displacement thickness δ^* with dimensionless longitudinal distance (x/c) for different pressure gradients. Figure (12) satisfies the Von Karman momentum equation (3). Figure (14) shows the variation of the shape factor H against the pressure gradient α at different stations. The shape factor H is the ratio between the displacement thickness and the momentum thickness θ .

The total drag coefficient or total drag force depends on the pressure gradient and the undisturbed velocity as shown in Fig. (15).

The total drag coefficient c_D is defined as:

$$c_D = \frac{D}{\frac{1}{2} u_\infty^2 \rho L c}$$

where D is the Drag force

u_∞ is the undisturbed velocity, upstream of the airfoil.

L span length and equal to 305 mm.

IV.3.9

c chord length and equal to 150 mm.

ρ density of air.

Thus, the total drag force can be computed from [9] according to the relation:

$$D = [(P_1 - P_2) + \rho u_{\infty}^2] A - \int_A \rho u^2 dA$$

where P_1 is the static pressure upstream of the airfoil.

P_2 is the static pressure at the first station.

A area of the cross-section of the wind tunnel at which the airfoil is located.

u is the velocity after the trailing edge.

CONCLUSIONS:

- 1) The velocity distribution at positive pressure gradient is flatter than zero-pressure gradient. This flatness increases with the increase of pressure gradient. But at negative pressure gradients the velocity distribution is shaper than that at zero-pressure gradient case.
- 2) For the same undisturbed velocity and distance from the trailing edge, the wake depth increases as the positive pressure gradient increases, till equal 14° and then slightly decreases with the increase of the pressure gradient. As the negative pressure gradient increases, the wake depth decreases sharply. Also the wake depth decreases as the distance from the trailing edge increases.
- 3) At positive pressure gradients, the wake width increases with increasing the positive pressure gradient and decreases with increasing the negative pressure gradient. Also the wake width increases with increasing the distance from the trailing edge.

- 4) At the same undisturbed velocity and distance from the trailing edge, the displacement thickness and the momentum thickness increases, at the positive pressure gradient increases, but it decrease slightly as the negative pressure gradient increases. Therefore the momentum losses at positive pressure gradient is greater than the losses at negative pressure gradient.
- 5) The drag coefficient depends on the pressure gradient and the undisturbed velocity. For the same undisturbed velocity, the total drag coefficient slightly decreases with the increasing of the positive pressure gradient and sharply increases with the increasing of the negative pressure gradient.

REFERENCES

- [1] Werle, M.J. and J.M. Verdon: "Viscid-Inviscid Interaction Analysis for Symmetric Trailing Edges". Report of United Technologies Research Centre, No. R 79-914493-5, p.74, 1979.
- [2] Schlichting, H.: "Boundary Layer Theory" Six th Edition. Mc-Grow Hill Book Company, New York 1968.
- [3] Townsend, A.A.: "Momentum and Energy Diffusion in the Turbulent Wake of a Cylinder" Proc. Roy Soc, (London) Ser. A, Vol. 197, No. A 1048 pp (124-140) May 11, 1948.
- [4] Kmo, Y.H. and Baldwin, L.V.: "Diffusion and Decay of Turbulent Elliptic Wakes" AJAA Journal Vol. 4, No. 9, p. 1566 September 1966.
- [5] Plothin, A. and Flugge-Lotz, I: "Anumerical Solution for the Laminar Wake Behind a Finite Plate Plate" J. of Applied Mechanics, p. 625 December 1968.
- [6] Counihan, J., Hunit, J.C.R. and P.S. Jackson "Wakes Behind Two-Dimensional Surface obstacles in Turbulent Boundary Layers" Journal Fluid Mech., Vol. 64, p.p 529-563, 1974.

- [7] Kearney, M.E. "A Hot-wire Anemometer Study of Free Turbulent Mixing in Axial Pressure Gradients". M.S. Thesis U.S. Naval Postgraduate School Monterey, Calif, Dec. 1972.
- [8] Hill, P.G., Schaut, U.W. and Senov, Y., "Turbulent Wakes in Pressure Gradients" Journal of Applied Mechanics, p. 518, December 1963.
- [9] Alan, L. Prasuhn: "Fundamentals of Fluid Mechanics" First Edition, Prentice-Hall, INC., Englewood Cliffs, New Jersey 07632, 1980.

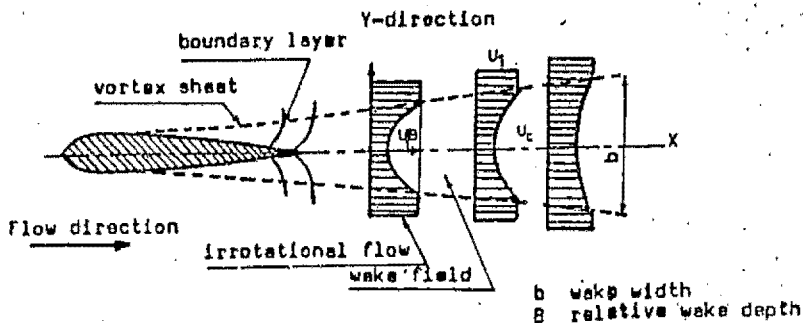


Fig.1 Illustration of flow in wake.

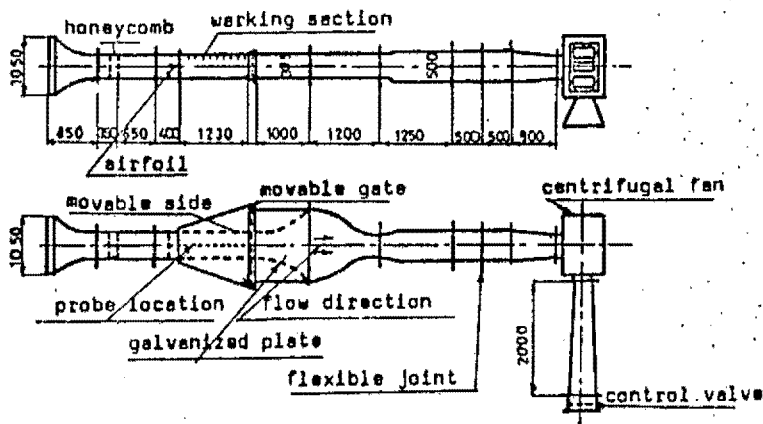


Fig.2 Wind Tunnel (Dimension in mm) .

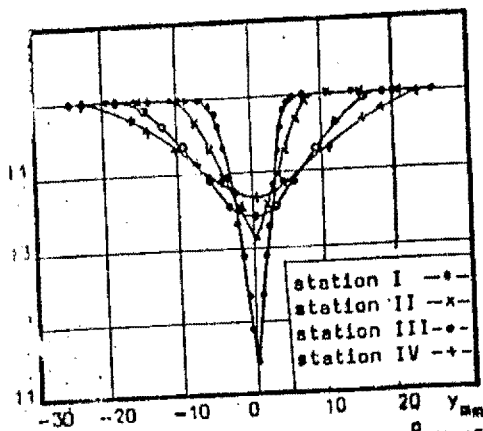


Fig. 3 Velocity profiles at $\alpha = 0^\circ$ and $U_\infty = 15$ m/s

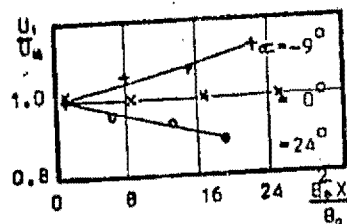


Fig. 6 Free stream velocity distribution at $U_\infty = 15$ m/s.

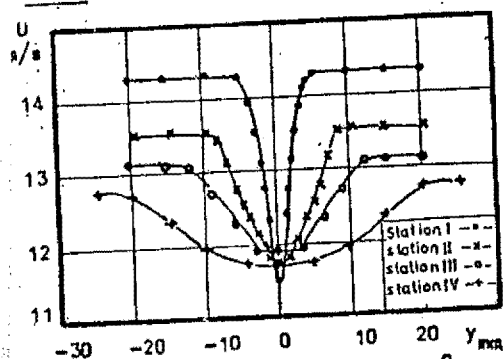


Fig. 4 Velocity profiles at $\alpha = 24^\circ$ and $U_\infty = 15$ m/s.

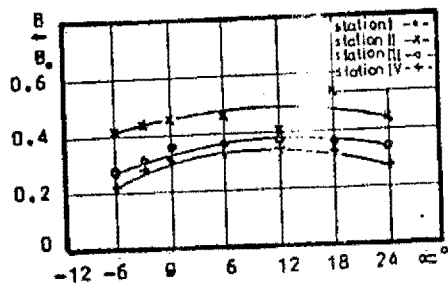


Fig. 7 Variation of wake depth with α at $U_\infty = 20$ m/s.

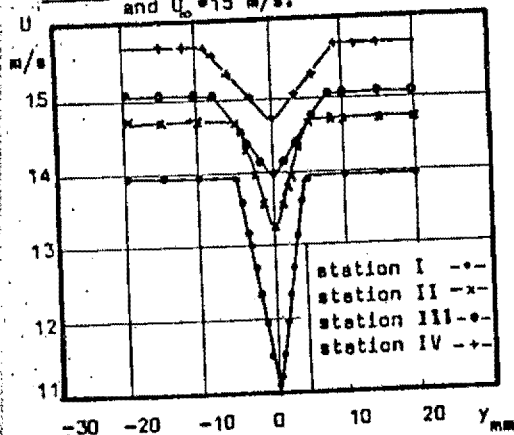


Fig. 5 Velocity profiles at $\alpha = -9^\circ$ and $U_\infty = 15$ m/s

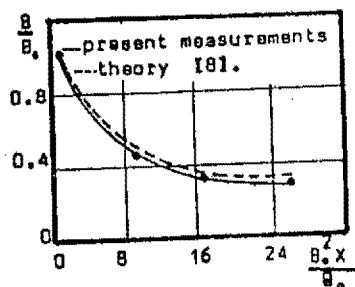


Fig. 8 Variation of relative wake depth with x at $\alpha = 24^\circ$ and $U_\infty = 20$ m/s

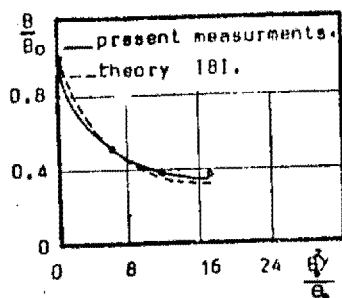


Fig. 9 Variation of relative wake depth with X at $\alpha = 0^\circ$ and $U_\infty = 20$ m/s 121.

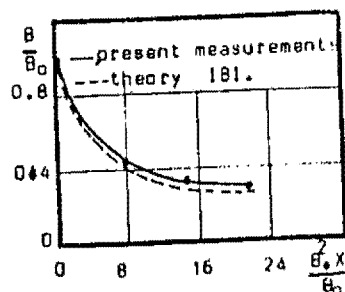


Fig. 10 Variation of relative wake depth with X at $\alpha = -12^\circ$ & $U_\infty = 12.5$ m/s 121.

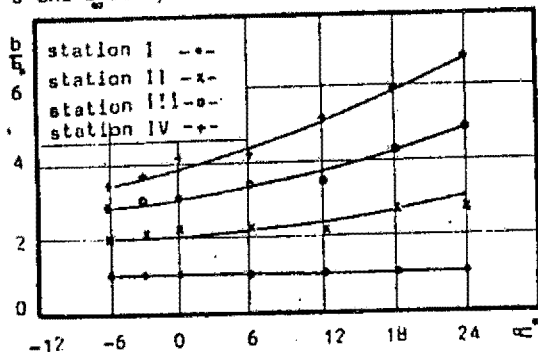


Fig. 11 Variation of relative wake width with α at $U_\infty = 20$ m/s.

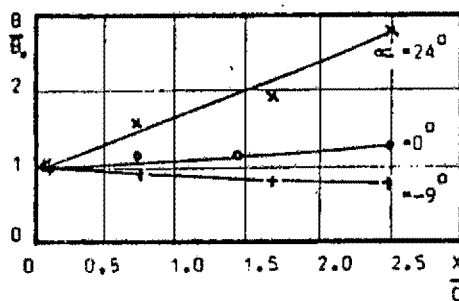


Fig. 12 Variations of momentum thickness at $U_\infty = 15$ m/s.

IV.3.14

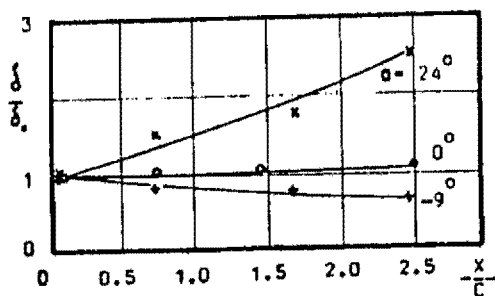


Fig. 13 Variation of displacement thickness at $U_\infty = 1.5$ m/s.

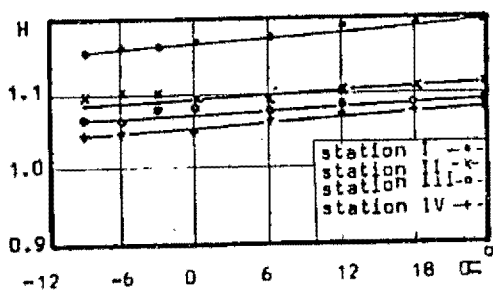


Fig. 14 Variation of shape factor with α at $U_\infty = 15$ m/s.

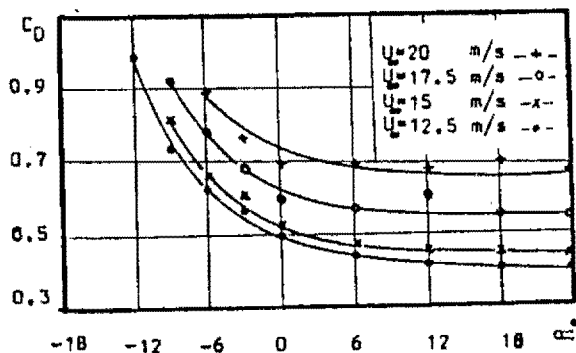


Fig. 15 Variation of drag coefficient with α